Dilp8 requires the neuronal relaxin receptor Lgr3 to couple growth to developmental timing

Andres Garelli[1,2,4,5], Fabiana Heredia[1,4], Andreia P. Casimiro[1,4], Andre Macedo[1], Catarina Nunes[1], Takashi Koyama[3], Alisson M. Gontijo[1,5]

[1] *Integrative Biomedicine Laboratory, CEDOC - Chronic Diseases Research Center, NOVA Medical School | Faculdade de Ciencias Medicas, NOVA University of Lisbon, Lisbon, Portugal.*
[2] *Instituto de Investigaciones Bioquímicas (INIBIBB), CONICET and Universidad Nacional del Sur, Bahía Blanca, Argentina.*
[3] *Development, Evolution and the Environment Laboratory, Instituto Gulbenkian de Ciência, Oeiras, Portugal.*
[4] *These authors contributed equally to this work.*
[5] *Corresponding authors agarelli@criba.edu.ar ; alisson.gontijo@fcm.unl.pt*

Abstract

How different organs in the body sense growth perturbations in distant tissues to coordinate their size during development is poorly understood. Here, we mutated an invertebrate orphan relaxin receptor, the *Drosophila Lgr3*, and found body asymmetries similar to those found in insulin/relaxin-like peptide 8 (*dilp8*) mutants, which fail to coordinate growth with developmental timing. Indeed, mutation or RNAi against *Lgr3* suppresses the delay in pupariation induced by imaginal disc growth perturbation or ectopic Dilp8 expression. By fluorescently-tagging the endogenous Lgr3 protein and performing CNS-specific RNAi, we find that Lgr3 is expressed and required in a novel subset of CNS neurons to couple growth to developmental timing. Our work sheds new light on the function and evolution of relaxin receptors and reveals a novel neuroendocrine circuit responsive to growth aberrations.

Main text

How different organs in the body sense growth perturbations in distant tissues to coordinate their size and differentiation status during development is poorly understood (*1, 2*). We have previously discovered a hormone in *Drosophila*, the insulin/relaxin-like peptide Dilp8, that ensures organ and body size coordination (*3*). In developing larvae, Dilp8 is produced and secreted from abnormally-growing imaginal discs. Its activity transiently delays the onset of metamorphosis by inhibiting the biosynthesis of the major insect molting hormone ecdysone by the prothoracic gland, a part of a compound endocrine structure called the ring gland (*3, 4*; Fig. 1A). Loss of *dilp8* uncouples the endocrine communication between imaginal discs and the prothoracic gland, making *dilp8* mutants susceptible to uncoordinated disc growth. This results in an increase in random deviations from

bilateral symmetry [fluctuating asymmetry (FA)], measurable at the population level (*3*). These findings have placed Dilp8 as a central player in the interorgan communication system that mediates plasticity to promote developmental stability in *Drosophila*. However, which molecule(s) and tissue(s) directly sense and/or transmit this abnormal growth signal to the prothoracic gland are unknown.

Type C1 Leucine-rich repeat-containing G-protein coupled receptors (Lgrs) are a highly conserved protein family in metazoans that act as receptors for insulin-like peptides of the relaxin subfamily in vertebrates, where they play diverse roles in tissue homeostasis and remodelling, behavior and reproduction (*5*). In invertebrates, however, they are considered orphan receptors and their biological function is unknown (5-7). The *Drosophila* genome encodes two orphan receptors, Lgr3 and Lgr4, with clear homologies to vertebrate relaxin receptors [~45% and ~40% sequence similarity to human, RXFP1/2, respectively (*6, 7*)]. To start untangling the function of relaxin receptors, we remobilized a MB Minos element (*8*) to generate a mutant in the *Drosophila* Lgr3 (Fig. 1B). The obtained imprecise excision allele was named *Lgr3[ag1].* Three precise excisions (*Lgr3[+/+]*) were also retained and used as genetic background controls. The *Lgr3[ag1]* imprecise excision (fig. S1) consists of a 3.8-kb deletion that completely removes the coding exon 7 and partially removes coding exon 8 (Fig. 1B). Reverse-transcriptase polymerase chain reaction assays followed by Sanger sequencing determined that the *Lgr3[ag1]* deletion leads to readthrough from exon 6 directly into intron 6 and usage of an aberrant splicing donor within intron 6 directly into exon 8 (Fig. 1B and fig. S2). The resulting transcript therefore has an intron-encoded premature termination codon (PTC) that truncates the Lgr3 protein one amino-acid after D_{326} (Fig. 1C). We conclude that *Lgr3[ag1]* encodes a severely compromised protein that is unlikely to bind ligand or signal due to a truncated ligand-binding LRR domain (*5*), and absence of the seven transmembrane (7TM) domains and G protein coupling Carboxy terminus (Fig. 1C).

While *Lgr3[ag1]* mutants are as viable and fertile as their *Lgr3[+/+]* genetic background controls (fig. S3), we noticed increased FA in *Lgr3[ag1]* adults wings. FA indexes (FAi) are increased by an order of ~3 when compared to their *Lgr3[+/+]* controls [$p = 0.002$ F-test for wing area FAi (Fig. 1D)]. This phenotype is indicative of uncoordinated imaginal disc growth during the larval stage, when wing size is determined, and is reminiscent of the increased FA phenotype of animals lacking the insulin/relaxin-like peptide Dilp8 (*3*). We thus hypothesized that Lgr3 and Dilp8 act on the same pathway to promote developmental stability by coupling imaginal disc growth to developmental timing.

To test the hypothesis that Lgr3 and Dilp8 are in the same pathway, we asked the question whether *Lgr3* mutants show a similar defect as *dilp8* mutants in the ability to delay the onset of metamorphosis in response to induced abnormal tissue growth (*3, 4*). We did this by inducing tissue damage in an *Lgr3[ag1]* background and carried out pupariation timing assays. Tissue

damage was induced by placing the proapoptotic gene *reaper* (*rpr*) under control of the wing-pouch *Beadex-Gal4* (*Bx>*) (*3, 6*), a combination that effectively caused a 66.7 ± 4.5-*h* (average ± SEM) delay in pupariation in control *Lgr3[+/+]* animals (Fig. 2A). Strikingly, this delay was reduced by 52.6 ± 3.8 *h* in *Lgr3[ag1]* mutants (~80%, $p < 0.05$ across all percentile comparisons, Tukey HSD test; Fig. 2A). This result demonstrates that Lgr3, like Dilp8, is critical to mediate the communication between abnormally growing imaginal discs and the prothoracic gland. In this same context, Dilp8 has been shown to control pupariation timing by acting upstream of the production of *Prothoracicotropic hormone* (*PTTH*) by the PTTH-producing neurons in the brain (*3*), which innervate the prothoracic gland and dictate the timing of ecdysone biosynthesis (*1-4, 9, 10*). Importantly, *Lgr3[ag1]* larvae pupariated at the same time as *Lgr3[+/+]* animals in control conditions without any induced tissue damage (Fig. 2A and fig S4C), suggesting that Lgr3, similarly to Dilp8 (*3*), does not control normal pupariation timing in the absence of growth aberrations. These results strongly indicate that Lgr3 and Dilp8 act on the same pathway.

To test whether the Dilp8 activity is Lgr3 dependent, we tested if *Lgr3* was necessary for the developmental delay produced by ectopic Dilp8 expression in the absence of tissue growth abnormalities (*3, 4*). Constitutive expression of a *UAS-dilp8::3xFLAG* (*UAS-dilp8*) transgene (*3*) under the control of a ubiquitous driver, *tubulin-Gal4* (*tub>*) delays the onset of pupariation by 25.2 ± 2.5 *h* compared to controls ($p < 0.05$, Tukey-Kramer adjusted HSD test; Fig. 2B). In contrast, the Dilp8-dependent delay is completely suppressed when Lgr3 activity is reduced by concomitant RNAi knockdown (*11*) (Fig. 2B and fig. S5). We conclude that animals lacking the *Drosophila* relaxin receptor Lgr3 are insensitive to ectopically produced Dilp8.

To gain insight into the tissue and cellular expression pattern of *Lgr3* at the protein level, we used CRISPR/Cas9 mediated homologous repair (*12, 13*) to tag the endogenous Lgr3 protein at its Amino-terminus with superfolder green fluorescent protein (sfGFP; *14*; Fig. 3A-B and fig. S6). We obtained one allele, *Lgr3[ag5]*, hereafter named *sfGFP::Lgr3*, which contained an intact *Lgr3* coding sequence downstream of the sfGFP insertion (fig. S6). sfGFP::Lgr3 labels ~180 CNS cell bodies, consisting of ~40 cell bodies in the brain proper and ~140 in the ventral nerve cord (VNC) of 3rd instar larvae CNS (Fig. 3C). No other larval tissue apart from the CNS had detectable fluorescence or anti-GFP staining. This rules out the possibility that *Lgr3* cell-autonomously controls ecdysone biosynthesis in the prothoracic gland downstream of Dilp8. The effectiveness of *sfGFP::Lgr3* as a protein translation reporter was further confirmed by analyzing alleles with premature termination codon-inducing (PTC+) indels in the *Lgr3* coding region following the inserted *sfGFP* sequence (fig. S6). The PTCs effectively reduced sfGFP::Lgr3 expression to undetectable levels (Fig. 3C, bottom panel), demonstrating the reliability of the *sfGFP::Lgr3* endogenous protein reporter. Importantly, PTC+ alleles, but not the PTC- *allele ag5*, had a similar increase in the pupal length to width ratio as the deletion mutant *ag1* (fig. S4A-D), and again did

not influence pupariation timing (fig. S4E) corroborating the phenotype observed in the *Lgr3[ag1]* allele. These results strongly suggest that the Lgr3 protein acts in a subpopulation of CNS neurons.

Critically, we were also unable to detect sfGFP::Lgr3 expression in neurons directly innervating the ring gland (Fig. 3C), ruling out the possibility that Lgr3 neurons control developmental timing by direct cellular contact or synapsis with the ring gland, such as through PTTH-producing neurons (*10*), the insulin producing cells (IPCs) *(15*), or subesophageal serotonergic neurons (*16*), all of which have been shown to modulate developmental timing. This scenario suggests that the Lgr3-positive neurons represent a novel distinct cellular population that has not been previously linked to growth and developmental timing control. To gain further insight into how Lgr3 neurons transmit the Dilp8 signal to the prothoracic gland, we looked into the neuroanatomy of *sfGFP::Lgr3* in more detail. Notably, sfGFP::Lgr3 expression was not homogeneous in the ~180 CNS cell bodies. It was most strongly expressed in a single dorso-ventral pair of midline neurons located deep in the thoracic segment of the VNC (hereafter abbreviated to MIL neurons, for midline internal Lgr3 neurons), and in a pair of bilateral neurons localized in the anterior part of the pars intercerebralis (hereafter abbreviated to PIL neurons, for pars intercerebralis Lgr3 neurons) (Fig. 3C, arrows and 3D) and (Fig. 3C, arrows and 3E). Both MIL and PIL neurons express *sfGFP::Lgr3* and present their characteristic neuroanatomy already at the L1 stage (fig. S7). MIL neurons project their neurites ventrally and then anteriorly towards the brain, branching close to the base of the brain (fig. 3D). PIL neurons extend a single neurite centripetally into the neuropil that branches dorsally into highly arborized termini and ventrally into a slightly less arborized projection with a yet undetermined terminal branch (Fig. 3E). We noticed that the proximal arborizations of PIL neurons project to a region of the pars intercerebralis known to harbor the IPCs and anterior neurites from Dilp7-producing dorsal medial (DMA1; *17*) neurons projecting from the VNC. To verify this assumption, we co-stained *sfGFP::Lgr3* brains with anti-Dilp5 or anti-Dilp7 as markers for IPCs or DMA1 neurons, respectively. Our results show that PIL neuron proximal arborizations project towards the nearby IPC-bodies reaching them from immediately underneath, while the IPCs neurites extend through the PIL neuron arborization (Fig. 3F). PIL neurons also show an intimate association with the axonal projections of the Dilp7-producing DMA1 neurons (Fig. 3G), providing anatomical and possible functional context for an anterograde neuronal input for PIL neurons (considering that proximal branches are typically dendritic; *18*).

One way by which neurons interact with IPCs is by modulating insulin release. The close proximity between PIL neurons and IPCs prompted us to test whether Lgr3 could have a function regulating insulin release. To test this hypothesis we quantified the levels of the major IPC insulin Dilp2 (*19*) in *Lgr3[ag1]* and *Lgr3[+/+]* brains, yet found no statistically significant difference (fig.

S8A-B), suggesting that Lgr3 does not modulate insulin release in normal conditions. Consistent with this, *Lgr3[ag1]* animals achieved a similar weight as their controls (fig. S8C). The same results were found when comparing the CRISPR-generated PTC+ mutant allele *[ag8]* with its control (fig. S8D-F). Even though these results do not exclude the possibility that PIL neurons modulate IPC activity, the *Lgr3* mutant results are coherent with our previous finding that *dilp8* loss-of-function does not affect average body weight or size in the absence of imaginal disc damage (*3*), adding evidence towards a dedicated role for Lgr3 in the Dilp8 pathway .

The expression pattern of the sfGFP::Lgr3 reporter suggests that disrupting receptor function exclusively in the CNS should be sufficient to suppress the Dilp8-dependent delay in the onset of metamorphosis. To test this, we crossed the *Lgr3-IR-V22* RNAi line to the panneuronal CNS driver *elav-Gal4* (*elav>*) (Fig. 4A). We then raised the larvae in the presence or absence of the genotoxic agent ethylmethanosulfonate (EMS), which induces apoptosis, tissue damage/regeneration, an imaginal-disc specific Dilp8 upregulation and consequentially a robust delay in the onset of metamorphosis (*8*). Reducing *Lgr3* function with RNAi in the nervous system using *elav>* leads to complete suppression of the EMS-induced delay, as also observed with an ubiquitous knockdown [using *armadillo-Gal4 (arm>)*] (Fig. 4A). We conclude that *Lgr3* is required in the CNS, likely in one or more of the ~180 Lgr3-positive cells described above, to convey the Dilp8-dependent developmental delay.

According to heterologous studies in human cell lines *in vitro* (*7*), *Lgr3* is a constitutively active receptor. Even though our loss-of-function studies do not rule out constitutive activity, they are more consistent with a scenario where Lgr3 is activated by Dilp8 or other downstream Dilp8-dependent signals. We thus hypothesized increased Lgr3 levels would not lead to a delay. Alternatively, if Lgr3 were constitutively active, it would delay pupariation timing if ectopically expressed. To conduct this experiment, we constructed a *UAS-Lgr3* transgene and expressed it ubiquitously under the control of *arm>*. We find that the pupariation time profile of *arm>Lgr3* animals is indistinguishable from controls (Fig. 4B). This result argues against a simple explanation where Lgr3 is constitutively active (*7*). Instead, it is in line with our findings that, in the absence of tissue growth aberrations or ectopic Dilp8 expression, Lgr3 activity is not required to control the timing of the onset of metamorphosis. These results are coherent with a model where Lgr3 is activated either directly or indirectly by the Dilp8 signal and hints towards the existence of a dedicated tissue stress sensing pathway in *Drosophila*.

Different organs need to sense growth perturbations in distant tissues to coordinate their size and differentiation status during development (*1*). Here, we have determined that the sensing of peripheral growth perturbations requires a novel population of CNS neurons expressing the Lgr3 relaxin receptor. Neuronal Lgr3 is required for the transmission of the peripheral growth aberration signal, Dilp8, to the prothoracic gland, which controls the onset of metamorphosis and thereby the

cessation of imaginal disc growth (*1, 3, 4, 9, 20*; Fig. 4C). This work reveals a new Dilp8-Lgr3 pathway that is critical to ensure developmental stability in *Drosophila*. Our study opens many questions for further research, such as the determination of whether or not the interaction between Lgr3 and Dilp8 is direct, which of the Lgr3-positive neurons are activated during Dilp8 expression, and how these connect to the ring gland.

The similarities between the neuroendocrine mechanisms controlling the larval to pupal transition in *Drosophila* and the hypothalamic-pituitary axis in vertebrates has been highlighted (*2, 21*). The neurosecretory cell-rich pars intercerebralis, in which the Lgr3-expressing PIL neurons are located, has anatomical, developmental and functional analogies to the hypothalamus, the structure that integrates the vertebrate CNS to the endocrine system via the pituitary gland. Similarly, the *Drosophila* pars intercerebralis connects the CNS to the endocrine ring gland complex via neurosecretory cells (*22*) such as the IPCs (*15*, *22*). Both systems have roles in stress-response, energy metabolism, growth, water retention, and reproduction (*5, 21*). Lgr3-positive neurons, such as the PIL neurons described herein, are well positioned to modulate the activity of ring gland-innervating neurons during tissue stress events that trigger Dilp8 secretion from the periphery. As the timing of vertebrate developmental transitions, such as puberty, can also be altered by intrinsic and extrinsic factors affecting body growth, such as inflammatory disease and nutritional status (*2*), the exploration of the role of relaxin signaling in modulating the hypothalamic-pituitary axis is a promising area for research. This is highlighted by the fact that the hypothalamus expresses relaxin receptors, including the Lgr3-homologue, RXFP1, in mammals and fish (*5, 23*), suggesting that a central neuroendocrine role for relaxin receptors might have evolved before the vertebrate and invertebrate split. A candidate peptide to regulate hypothalamic-pituitary stress-responses via relaxin receptors is the neuropeptide Relaxin-3 (RLN3), which has been traditionally viewed as being the ancestor ligand for all vertebrate relaxins (*24, 25*). RLN3 is strongly expressed in stress-responsive neurons from the nucleus incertus (NI) that directly innervate and modulate hypothalamic activity (*5, 26-28*). Our results therefore reveal an unexpected and striking similarity between the Dilp8-Lgr3 pathway and the vertebrate relaxin signaling pathway and hint to an ancient stress-responsive pathway coordinating animal growth and maturation timing.

Acknowledgements

We thank C. Mirth, C. Ribeiro and A. Jacinto for their comments and suggestions; I. Miguel-Aliaga, A. Jacinto, P. Leopold, P. Domingos, C. Mirth, R. Teodoro and M. Dominguez for reagents. Stocks obtained from the Bloomington Drosophila Stock Center (NIH P40OD018537) and from the VDRC were used in this study. AMG, FH, AM and TK are supported by the FCT, under the FCT Investigator Programme and FCT fellowships SFRH/BPD/94112/2013, PD/BD/52421/2013 and

SFRH/BPD/74313/2010, respectively. AG is supported by the CONICET and UNS. The work in the laboratory of AMG is funded by the CEDOC and the European Commission FP7 (PCIG13-GA-2013-618847). AG thanks NP Rotstein and LE Politi for providing funds and space to develop part of this project in their lab.

References

1. A. W. Shingleton *Organogenesis* **6**, 76 (Apr-Jun 2010).
2. I. K. Hariharan *Sci Signal* **5**, pe27 (Jun 19, 2012).
3. A. Garelli, A. M. Gontijo, V. Miguela, E. Caparros, M. Dominguez, Science **336**, 579 (May 4, 2012).
4. J. Colombani, D. S. Andersen, P. Léopold, Science **336**, 582 (May 4, 2012).
5. R. A. Bathgate *et al.*, *Physiol Rev* **93**, 405 (Jan 2013).
6. M. B. Van Hiel, H. P. Vandersmissen, T. Van Loy, J. Vanden Broeck, Peptides. 34, 193 (Mar 2012).
7. M. B. Van Hiel, H. P. Vandersmissen, P. Proost, J. Vanden Broeck, Peptides. pii: S0196-9781(14)00214-9. doi: 10.1016/j.peptides.2014.07.014. (Jul 23, 2014)
8. A. Metaxakis, S. Oehler, A. Klinakis, C. Savakis, *Genetics* **171**, 571 (Oct 2005).
9. A. Halme, M. Cheng, I. K. Hariharan, *Curr Bio*l **20**, 458 (Mar 9, 2010).
10. Z. McBrayer *et al.*, *Dev Cell* **13**, 857 (Dec 2007).
11. G. Dietzl *et al.*, *Nature* **448**, 151 (Jul 12, 2007).
12. S. J. Gratz *et al.*, *Genetics* 194, 1029 (Apr 2013).
13. F. Port, H. M. Chen, T. Lee, S. L. Bullock. *Proc Natl Acad Sci U S A,* **111**, E2967 (Jun 22, 2014).
14. J. D. Pédelacq *et al., Nat Biotechnol* **24**, 79 (Jan 2006).
15. E. J. Rulifson, S. K. Kim, R. Nusse, *Science* **296**, 1118 (May 10, 2002).
16. Y. Shimada-Niwa, R. Niwa, *Nat Commun* **5**, 5778 (Dec 15, 2014).
17. I. Miguel-Aliaga, S. Thor, A. P. Gould, *PLoS Biol* **6**, e58 (Mar 11, 2008).
18. V. Hartenstein, S. Spindler, W. Pereanu, S. Fung, *Adv Exp Med Biol* **628**, 1 (2008).
19. C. Geminard, E. J. Rulifson, P. Leopold, *Cell Metab* **10**, 199 (Mar, 2009).
20. L. I. Gilbert, R. Rybczynski, J. T. Warren. *Annu Rev Entomol* **47**, 883 (2002).
21. B. de Velasco *et al.*, *Dev Biol* **302**, 309 (Feb 1, 2007).
22. T. Siegmund, G. Korge, *J Comp Neurol* **431,**481 (Mar 19, 2001).
23. A. Donizetti *et al.*, *Dev Growth Differ* **52**, 799 (Jan 2010).
24. T. N. Wilkinson, R. A, Bathgate. *Adv Exp Med Biol* **612**, 1 (2007).
25. S. Yegorov, S. Good, *PLoS One* **7**, e32923 (Mar 21, 2012).
26. B. M. McGowan *et al.*, *Am J Physiol Endocrinol Metab* **295**, E278 (Aug 2008).
27. Y. Watanabe, Y. Miyamoto, T. Matsuda, M. Tanaka, *J Mol Neurosci* **43**, 169 (Feb 2011).
28. B. M. McGowan *et al.*, *J Endocrinol* **221**, 337 (May 12, 2014).

Figure Legends

Fig. 1. Mutation in the *Drosophila* relaxin receptor Lgr3 leads to increased fluctuating asymmetry. (A) A neuroendocrine pathway coupling growth and developmental timing (*3, 4*). Scheme adapted from (*9*). **(B)** Remobilization of Minus element *MB06848* positioned between coding exons 6 and 7 of the *Lgr3* locus on Chromosome III generated a 3.8-kb deletion, named *Lgr3[ag1]*. **(C)** Scheme of predicted protein structure of the wild-type Lgr3 protein and the truncated Lgr3[ag1] protein based on vertebrate relaxin receptor structure data (*5*). Major domains are depicted: Low-density lipoprotein receptor domain class A (LDLa), Leucine-rich repeat (LRR), and seven transmembrane (7TM). The first TM/signal peptide (SP) domain is not predicted to be cleaved. The approximate region where *ag1* mutation truncates the Lgr3 protein is depicted. **(D)** Bar graphs of the FAi (*3*) of the area (left panel) and length (right panel) of the wing pairs of the genotypes indicated. Numbers (N) of the wing pairs scored. F-test *p* values are shown.

Fig. 2. Lgr3 couples imaginal disc growth to developmental timing by acting in the Dilp8 pathway. (A) Mutation of *Lgr3* abrogates interorgan communication between regenerating discs and the neuroendocrine centers coordinating the onset of metamorphosis. Expression of the proapoptotic gene *rpr* in the imaginal disc wing pouch under the control of *Bx>* leads to regeneration-dependent 66.7-h-delay in pupariation timing. Heat map bar graphs showing pupariation time (percentiles of pupae +/- SEM) of 5 repeats of the depicted genotypes. **(B)** *Lgr3* acts in the Dilp8 pathway. Two different RNAi lines against *Lgr3, UAS-Lgr3-IR[JF03217]* and *UAS-Lgr3-IR[GL01056]* [hereafter *Lgr3-IR-V10* and *Lgr3-IR-V22* (*V10* and *V22*)], suppress the delay caused by expression of Dilp8 under the control of the ubiquitous *tub>* driver. Shown are percentiles of pupae +/- SEM of 4-6 repeats of the depicted genotypes. Asterisks indicate $p<0.05$ against all other genotypes (ANOVA, Tukey-Kramer adjusted HSD test).

Fig. 3. Lgr3 is expressed in a subpopulation of CNS neurons. (A) Strategy used to generate a Lgr3 protein reporter. CRISPR/Cas9 mediated homologous repair (*13*) was used to integrate sfGFP in frame with exon 1 of *Lgr3.* This generated the protein reporter allele *ag5* (named as *sfGFP::Lgr3*), which does not contain indels in the exon 1 region, and alleles *ag6-8* which contain PTC+ indels (fig. S6). Two thin black lines indicate the sites of the CRISPR gRNAs used. **(B)** Lgr3 protein scheme depicting the approximate localization of the sfGFP insertion and the protein truncations caused by the PTC+ indel mutations (see also fig. S6). **(C)** Sum of confocal z-stack slices of the CNS of a 3rd instar larvae stained with anti-GFP (green) to show sfGFP::Lgr3 expression (green) and with anti-nc82 (magenta) and DAPI (blue) counterstains to show the synapses (neuropil) and nuclei, respectively. Arrows point to two bilateral pairs of PIL neurons (top) and to the MIL neurons in the midline of the VNC (bottom). MIL neurons are oriented dorso-

ventrally. Arrowheads point to the proximal projections of the PIL neurons. sfGFP::Lgr3 is also expressed in ~170 other cell bodies, but at a lower level than in PIL and MIL neurons. No anti-GFP staining is detectable in the CNS of an animal carrying a sfGFP::Lgr3 insertion with a PTC+ indel [*ag7*]. **(D)** MIL neuron cell bodies (cb) located deep in the VNC project ventrally and anteriorly (red arrowheads) for a short distance (red arrowheads). Adjacent anterior projections are depicted (blue arrows). **(E)** Rostral view of the pars intercerebralis depicting the PIL neurons stained with anti-GFP [green (left) and black (right)] and counterstained with DAPI (magenta). Possible proximal dendritic arborizations are indicated with red arrows. Blue arrows indicate a ramification, likely axonic, with an undetermined terminus. Primary neurites (red arrowhead). **(F)** PIL neurons associate closely to IPCs. Z-stack projection of confocal stacks stained with anti-GFP (green) and anti-Dilp5 (magenta). **(G)** PIL neurons associate closely to Dilp7-producing DMA1 neurons in the pars intercerebralis. Z-stack projection and orthogonal view of confocal stacks stained with anti-GFP (green) and anti-Dilp7 (magenta).

Fig. 4. Lgr3 is required in a novel subpopulation of CNS neurons to receive and transmit the Dilp8 signal to the ring gland. (A) Heat map bar graphs showing pupariation time (percentiles of pupae +/- SEM) of 3 repeats of larvae of the depicted genotypes fed either PBS (control) or the DNA-damaging agent, EMS (*3*). *arm>* drives ubiquitous expression while *elav>* drives CNS-specific expression. **(B)** *Lgr3* overexpression is not sufficient to delay the onset of metamorphosis. Heat map bar graphs showing pupariation time (percentiles of pupae +/- SEM) of 6 repeats of the depicted genotypes. Two *UAS-Lgr3* transgene insertions (*a* and *b*) were tested. $p>0.05$, ANOVA. **(C)** Cartoon depicting the Dilp8-Lgr3 abnormal tissue growth-sensing pathway. A yet uncharacterized neuronal circuitry acts likely upstream of the known PTTH and ring gland components to delay the larval to pupa transition.

Figure 1.

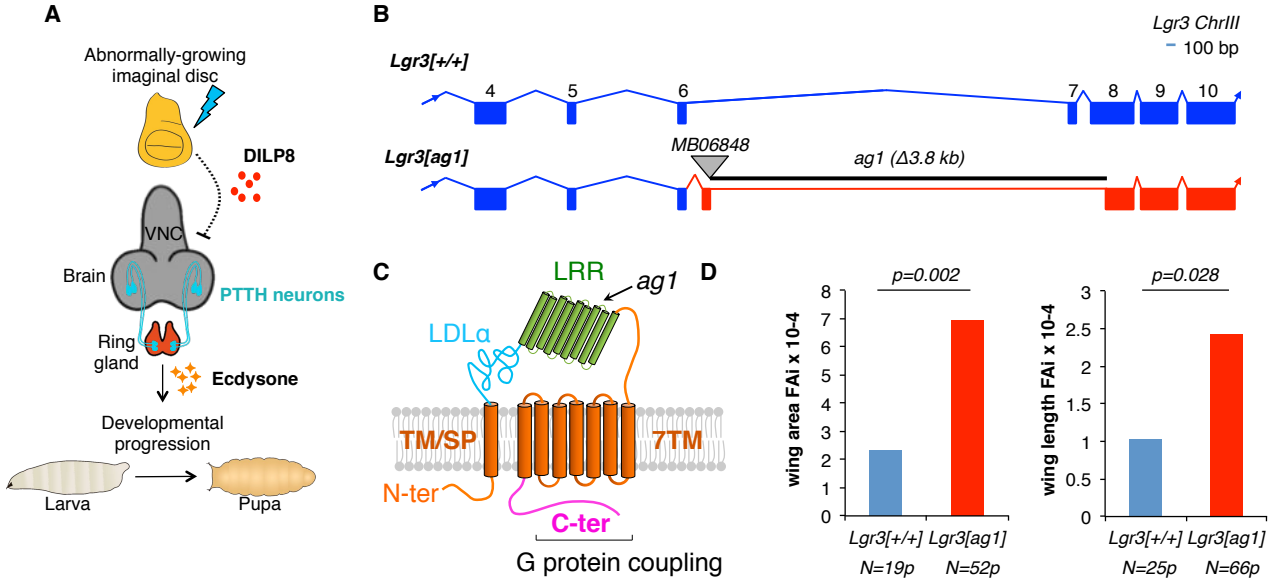
A
Abnormally-growing imaginal disc
DILP8
VNC
Brain
PTTH neurons
Ring gland
Ecdysone
Developmental progression
Larva
Pupa
B
Lgr3 ChrIII
100 bp
Lgr3[+/+]
4
5
6
7
8
9
10
Lgr3[ag1]
MB06848
ag1 (Δ3.8 kb)
C
LRR
ag1
LDLa
TM/SP
7TM
N-ter
C-ter
G protein coupling
D
p=0.002
wing area FAi x 10-4
Lgr3[+/+]
Lgr3[ag1]
N=19p
N=52p
p=0.028
wing length FAi x 10-4
Lgr3[+/+]
Lgr3[ag1]
N=25p
N=66p

Figure 2.

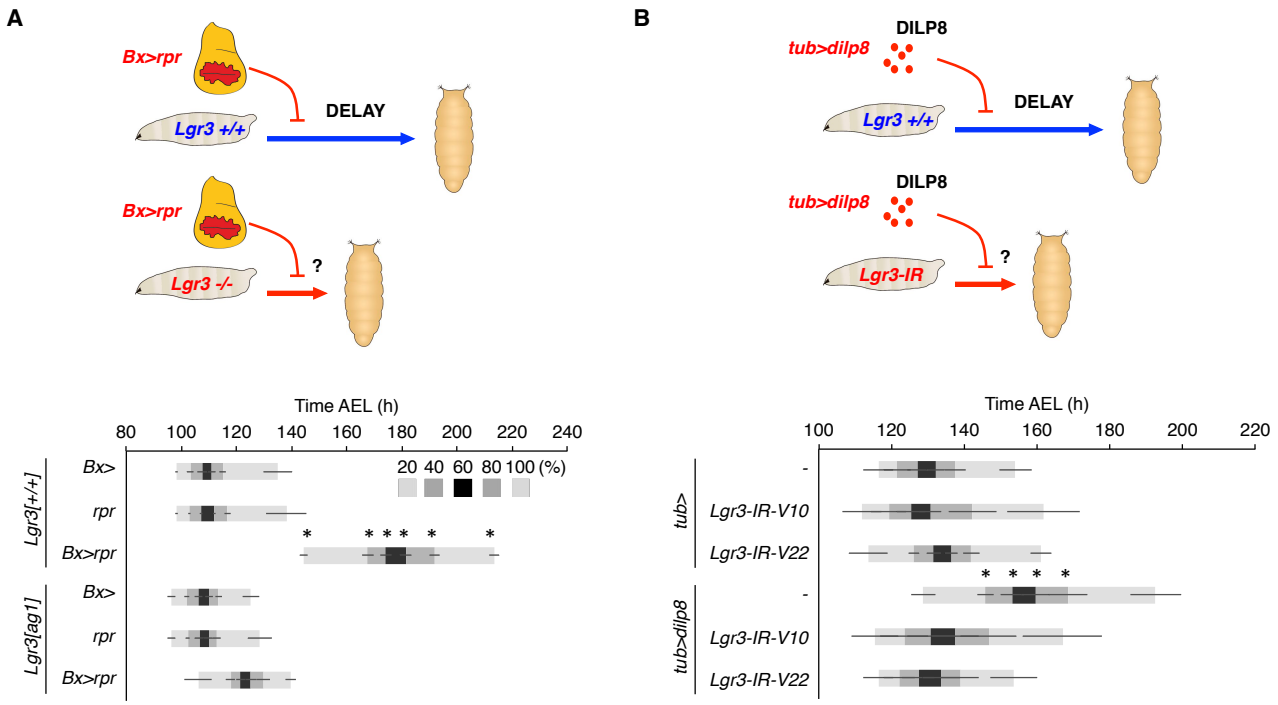
A
Bx>rpr
Lgr3 +/+
DELAY
Bx>rpr
Lgr3 -/-
?
Time AEL (h)
80 100 120 140 160 180 200 220 240
20 40 60 80 100 (%)
Lgr3[+/+]
Bx>
rpr
Bx>rpr
Lgr3[ag1]
Bx>
rpr
Bx>rpr
B
DILP8
tub>dilp8
Lgr3 +/+
DELAY
DILP8
tub>dilp8
Lgr3-IR
?
Time AEL (h)
100 120 140 160 180 200 220
tub>
-
Lgr3-IR-V10
Lgr3-IR-V22
tub>dilp8
-
Lgr3-IR-V10
Lgr3-IR-V22

Figure 3.

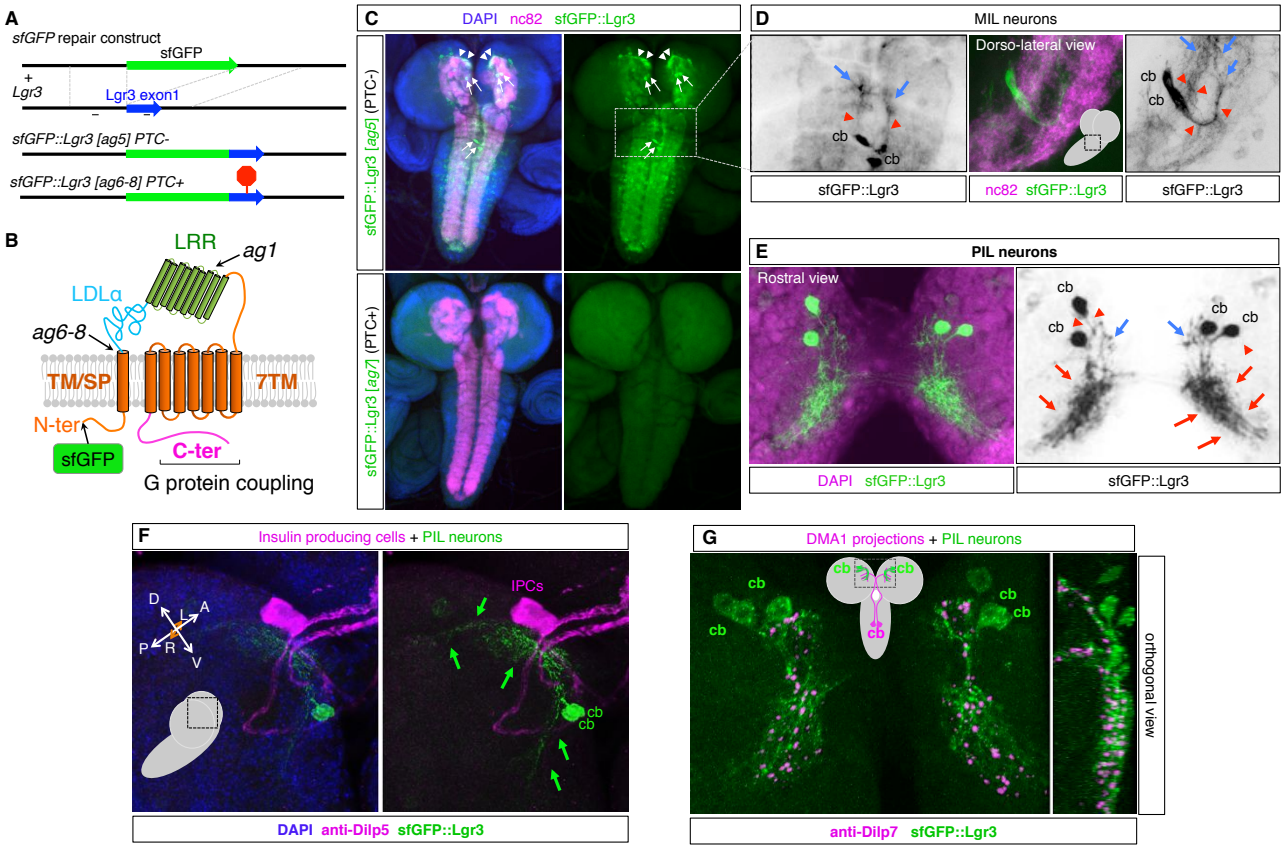
A
sfGFP repair construct
sfGFP
+
Lgr3
Lgr3 exon1
sfGFP::Lgr3 [ag5] PTC-
sfGFP::Lgr3 [ag6-8] PTC+
B
LRR
ag1
LDLa
ag6-8
TM/SP
7TM
N-ter
sfGFP
C-ter
G protein coupling
C
DAPI nc82 sfGFP::Lgr3
sfGFP::Lgr3 [ag5] (PTC-)
sfGFP::Lgr3 [ag7] (PTC+)
D
MIL neurons
Dorso-lateral view
cb
sfGFP::Lgr3
nc82 sfGFP::Lgr3
sfGFP::Lgr3
E
PIL neurons
Rostral view
DAPI sfGFP::Lgr3
sfGFP::Lgr3
F
Insulin producing cells + PIL neurons
D
A
P
R
V
IPCs
cb
DAPI anti-Dilp5 sfGFP::Lgr3
G
DMA1 projections + PIL neurons
orthogonal view
anti-Dilp7 sfGFP::Lgr3

Figure 4.

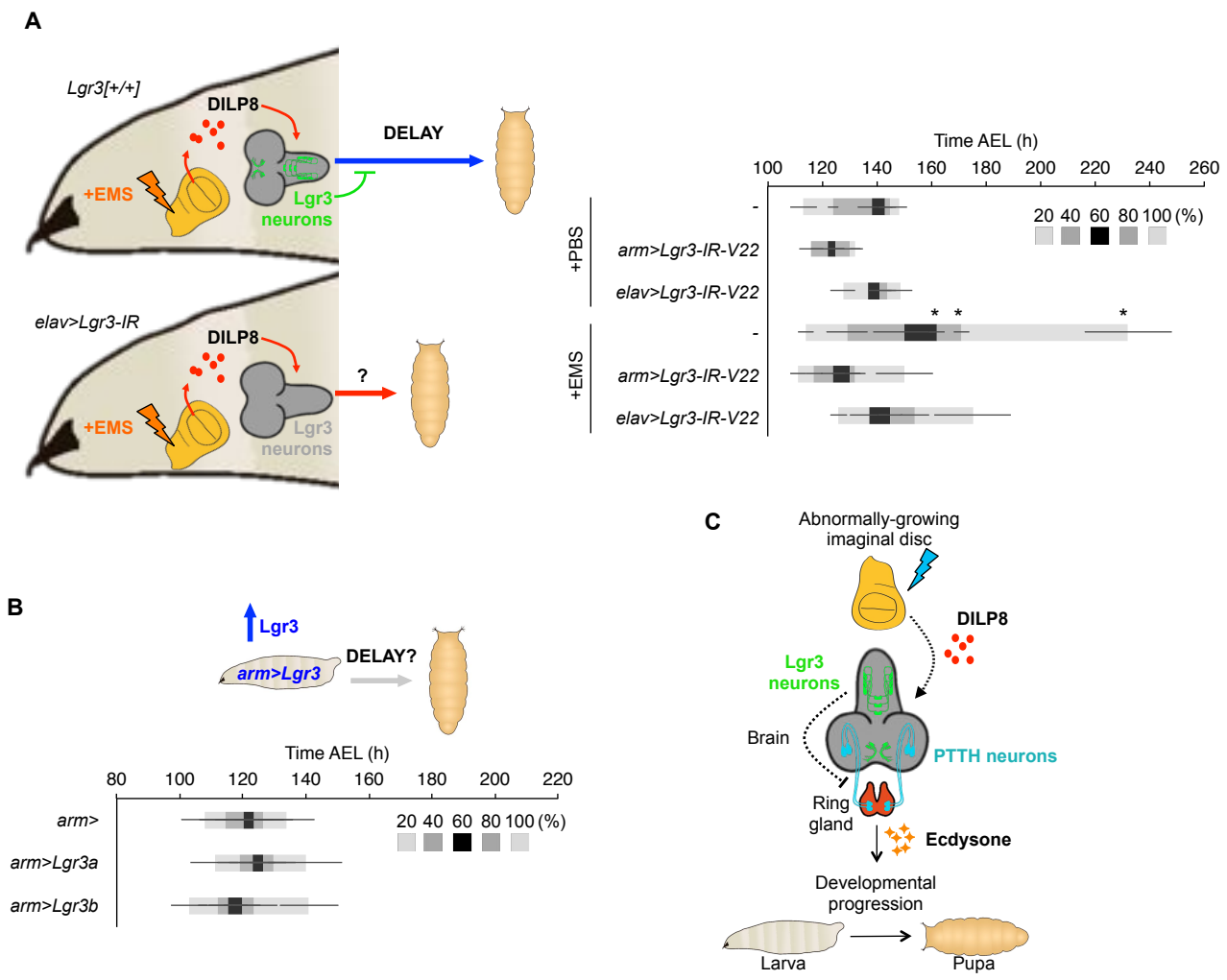
A
Lgr3[+/+]
DILP8
+EMS
Lgr3
neurons
DELAY
elav>Lgr3-IR
DILP8
+EMS
Lgr3
neurons
?
Time AEL (h)
100 120 140 160 180 200 220 240 260
20 40 60 80 100 (%)
+PBS
-
arm>Lgr3-IR-V22
elav>Lgr3-IR-V22
+EMS
-
arm>Lgr3-IR-V22
elav>Lgr3-IR-V22
B
Lgr3
arm>Lgr3
DELAY?
Time AEL (h)
80 100 120 140 160 180 200 220
20 40 60 80 100 (%)
arm>
arm>Lgr3a
arm>Lgr3b
C
Abnormally-growing
imaginal disc
DILP8
Lgr3
neurons
Brain
PTTH neurons
Ring
gland
Ecdysone
Developmental
progression
Larva
Pupa